参赛队员姓名：周胤成、王潇远、王石

中学：南京外国语学校

省份：江苏省

国家/地区：中 国

指导教师姓名：何 亮

指导教师单位：南京大学

论文题目：Hearing Light—Photoacoustic Effect of a Jar and its Thermodynamic Characteristics

# Hearing Light—Photoacoustic Effect of a Jar and its Thermodynamic Characteristics

*by Zhou Yincheng, Wang Xiaoyuan, Wang Shi*

## Abstract

This paper explores a phenomenon we called "Hearing Light.” By passing an AC current through an incandescent light bulb, shinning the emitted light onto a glass jar with half of its inside covered by black carbons and a hole in its cap, a sound can be detected by a microphone.

Experiments to demonstrate the phenomenon are detailed and successful recreation of the auditory effect is achieved. The observed phenomenon is called photoacoustic effect. This entails the conversion of AC electricity into chopped light (oscillating light intensity), which triggers intermittent compression and expansion of the gas within the jar, resulting in sound generation.

Quantitative theoretical analysis is then provided. First, models are developed for both the light bulb, the carbon covered jar and the adjacent air. Then, assessment of factors such as incident light, heat transformation, temperature distribution, and the mechanic movement of the air have been comprehensively discussed. At the end, our theoretical model quantitatively explained all the experimental results, perfectly.

This paper concluded that the sound intensity rises with the rise of light intensity and decreases with the increase of the distance. Surprisingly, the sound intensity is also linearly proportional to the ratio between the carbon area and the hole area. Most importantly, the frequency of the sound is double the AC frequency.

Key words: photoacoustic effect, auditory effect, optical absorption, oscillating light intensity, heat transformation, temperature distribution

# Table of Contents

# I. Introduction

We all know that eyes are needed to see light and ears are needed to hear sound. Recently, we have read an experiment of **seeing the sound** by the putting small sands on a drum to demonstrate the standing wave. Beautiful patterns can be seen for particular frequencies. Thus, we are curious of this question. Can the light be heard?

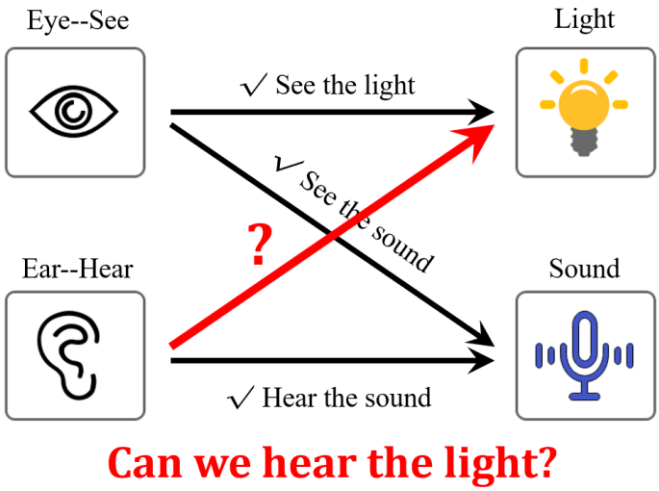


Figure 1.1. Can we hear the light?

In this paper, we have explored a phenomenon called “Hearing Light”. Here, by a very simple experimental setup, light can be converted into sound and heard by a microphone.

The explanation of this phenomenon, known as the photoacoustic effect, has captured the interests of researchers since its initial exploration in 1880[1]. Over time, the photoacoustic effect has been explored by various scientists, yielding significant insights into its underlying principles. “The Theory of the Photoacoustic Effect with Solids” [2] delves into the acoustic signals generated when chopped light impinges on a solid in an enclosed cell. This theory provides a foundation for the emerging field of photoacoustic spectroscopy, allowing the acquisition of optical absorption spectra for otherwise optically opaque materials.

Here, we have built an experimental setup using a 200 walt incandescent light bulb,

a glass jar with half of its inside covered by black carbons and a hole in its cap, and a microphone. By turning on the AC power from the household outlet, the light is emitted from the light bulb and a sound with twice the frequency of the AC power can be detected by a microphone. The key parameters including light intensity, distance, and diameter of the hole, which influence the intensity of the sound have been systematically studied. Furthermore, a comprehensive physical model has been built based on qualitative and quantitative analysis. All the experimental results can be explained and quantitively consistent with our theoretical model.

# II. Experiment

## 2.1 Experimental setup

Figure 2.1(a) demonstrates the schematic diagram of our experimental setup, which includes a 200 walt incandescent bulb, a glass jar, and a microphone. The incandescent bulb was connected to the household AC power source ($f = 50\ Hz$).

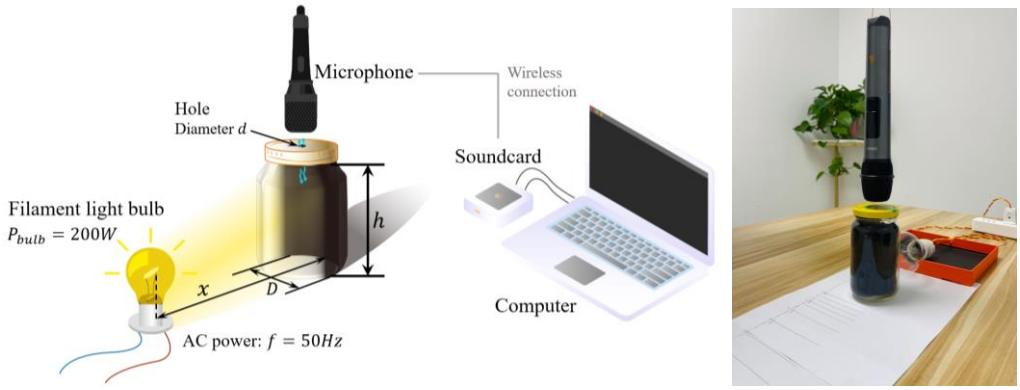


Figure 2.1 a) Schematic diagram of the experimental setup. b) The light bulb, the jar and the microphone.

Figure 2.2. Discussion of the experiment.

Figure 2.3 The sound card on the left, connected to a computer.

Inside the jar, half of it has been covered by carbon particles produced by burning candles. Holes with different sizes have been drilled by an electric drill onto the caps of the jar. The distance between the light bulb and the carbon layer is also controlled and measured by a ruler as shown in Figure 2.1(b).

We put a microphone on top of the jar to acquire the sound. The microphone is connected to a soundcard (Yamaha UR12) in another room which is called data processing room shown in Figure 2.3. Such card can transfer the sound collected by the microphone to the computer. GarageBand has been used to record the sound onto the computer. And the data have been processed by Adobe Audition and MATLAB.

Three sets of experiments have been performed. Experiment I: adjust the size of the holes on the caps. Experiment II: adjust the power of the bulb by a voltage transformer. Experiment III: adjust the distance between the light bulb and the carbon layers.

As shown in Figure 2.1(a), key parameters have been marked, including: the inner diameter of the glass jar ($D$), the height of the carbon layer inside the jar ($h$), the diameter of the hole ($d$), the power of the bulb ($P_{bulb}$), the distance of the tungsten filament to the carbon ($x$). Several jars and caps with different size of holes have been used as shown in Figure 2.4


Figure 2.4: Part of the jars and caps with different hole diameter used in the experiments.

Figure 2.5(a) exhibits the original recorded sound. A magnified data are shown in Figure 2.5(b). A strong sound of 100 Hz can be observed as soon as the lamp is turned on at t = 20 s.

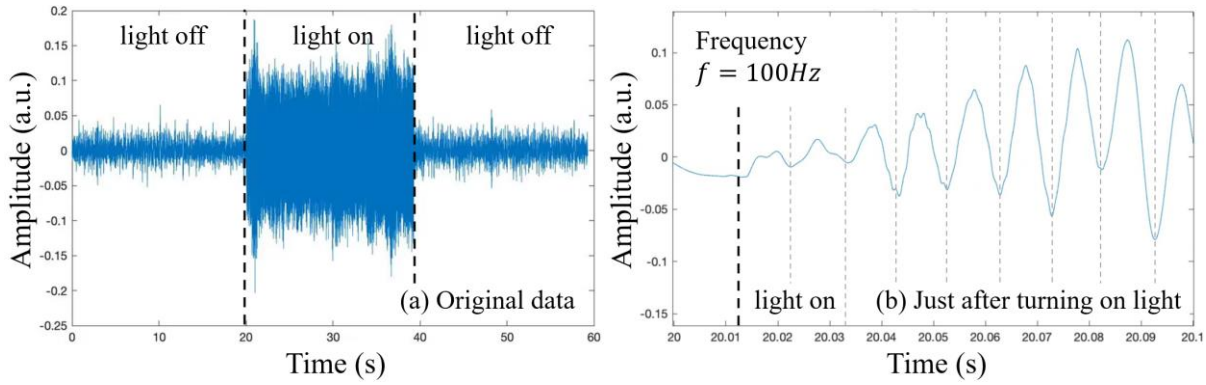


Figure 2.5. (a) The original recorded sound. (b) The zoom-in view at 20 s when the lamp is turned on. Clearly sound of 100 Hz can be seen.

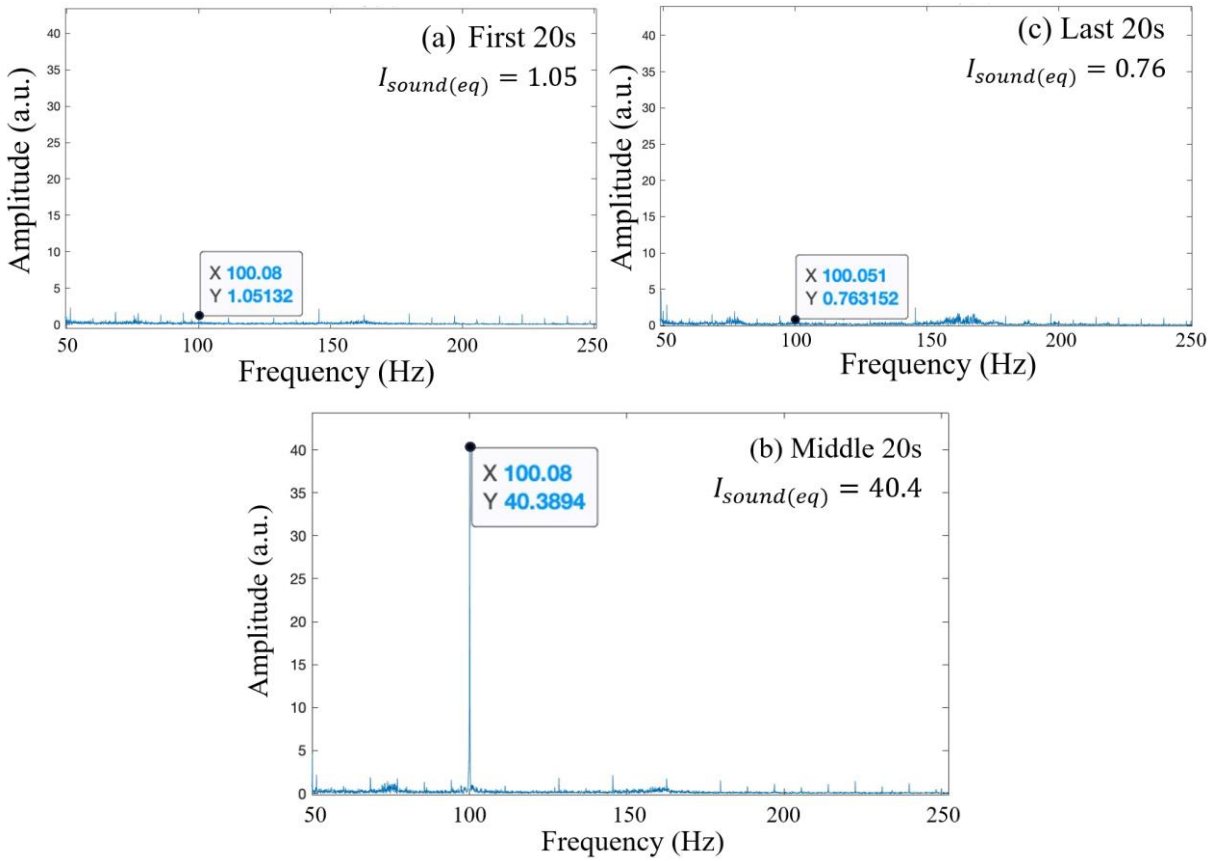


Figure 2.6 The FFT of the first 20s (a), the middle 20s (b) and the last 20s (c) sounds.

As shown in Figure 2.5, during each experiment, 20 seconds of sound without the light has been recorded which gives the background noise. Then, we turn on the AC

power, let the light emitted from the incandescent bulb to illuminate the carbon layer and record the sound for anther 20s. After turning off the light, we keep recording the sound of the environment for an extra 20 seconds and check if there is any difference of the background noise. If there is some obvious discrepancy between the first and second recorded background noise, we will do the experiment again. It is necessary to control the background noise lower than -90 dB, which is 2 orders of magnitude smaller than the signal. Thus, the background sounds can be neglected during analysis.

fft.m

```
syms y fs;
syms in_put;
in_put= 'C:\Users\zhouz\Desktop\Hearing Light\Sound\5*7 1.85.mp3';
[y,fs] = audioread(in_put);
info=audioinfo(in_put)  ;
sound(y,fs);
T=1/fs;
t=(0:length(y)-1)*T;
f=(0:length(y)-1)*fs/length(y);
figure(1);
yz=y(:,1);
subplot(2,2,3);
n=length(yz);
y1=fft(yz,n);
F=fs/length(yz);

plot(f,abs(y1));
title('original information');
ylabel('H(jw)');
xlabel('F(Hz)');
subplot(2,2,4);
n2=length(yz2);
y1=fft(yz2,n2);
F=fs/length(yz2);
```

Figure 2.7 MATLAB code for FFT

After collecting the 1-minute-long audio (Figure 2.5), we have done Fast Fourier Transfer (FFT) by MATLAB to the recorded sound. Figure 2.7 shows the code of the FFT, while Figure 2.6 exhibits the spectrums of the audio of the three sections after FFT. We have collected the amplitude of 100Hz in the transformed spectrum (Figure 2.6c) to represent the sound intensity of certain parameters.

## 2.2 Experiment I: Intensity vs. size of the hole

To investigate the influence of the diameter of the hole on sound intensity, we have selected three containers of different sizes, each equipped with a cap containing a hole

of various diameters as shown in Table 2.1. The bulb power of 200W @ 50 Hz and filament-to-carbon layer distance of 11cm have been fixed.

| $D$(cm) | $h$(cm) | $d$(mm) | Sound intensity (a. u.) |
|---|---|---|---|
| 7 | 11 | 1 | 7.8 |
| | | 1.85 | 13.3 |
| | | 2.5 | 20.6 |
| | | 3.15 | 110.7 |
| | | 4.4 | 46.1 |
| | | 5.2 | 35.5 |
| | | 6.35 | 31.8 |
| | | 7 | 24.5 |
| 10.5 | 11 | 1 | 16.0 |
| | | 2 | 30.5 |
| | | 3 | 181.5 |
| | | 4 | 94.6 |
| | | 5 | 60.2 |
| | | 6 | 38.9 |
| | | 7 | 34.8 |
| | | 8 | 20.2 |
| 5 | 7 | 1 | 3.2 |
| | | 1.85 | 7.7 |
| | | 2.5 | 12.9 |
| | | 3.15 | 52.6 |
| | | 4.4 | 34.9 |
| | | 5.2 | 24.8 |
| | | 6.35 | 21.6 |
| | | 7 | 19.6 |

Table 2.1 Experimental data

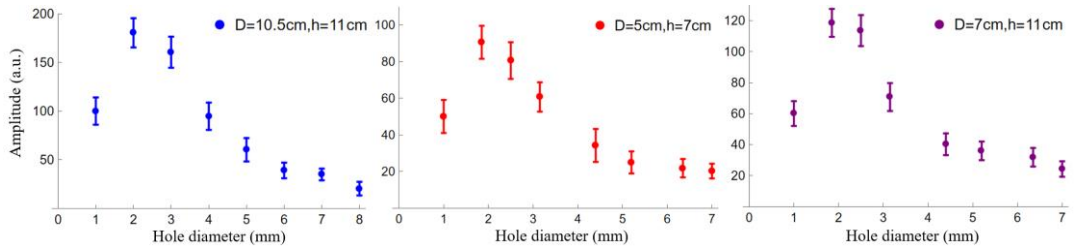


Figure 2.8: Experimental data

As shown in Figure 2.8, all the data from three sets of jars have similar patterns. Initially, sound intensity increases with increasing hole size, it reaches a maximum

value and subsequently decreases with further increases in hole size. This phenomenon can be understood as the following:

If the hole diameter is too small, the flow of gas during the expansion-contraction process inside the container might be severely restricted. This could result in minimal sound pressure changes near the hole, leading to lower sound intensity. Additionally, excessively small holes could cause scattering and attenuation of sound waves as they pass through. Due to the small diameter, sound waves passing through the hole might interact with the edges, causing part of its energy being scattered into other directions, thus diminishing the sound intensity.

On the other hand, if the hole diameter is too large, noticeable expansion-contraction process of the gas cannot form beside the hole because the velocity of air passing through the hole decreases. Thus, oversized holes will prevent the formation of significant sound pressure changes near the hole, consequently affecting sound intensity.

In summary, there exists an optimal size where gas flow around the hole generates the maximum sound. Container size also acts as a variable influencing sound intensity, and each container corresponds to a different optimal size.

Further analysis of the data reveals that sound intensity is proportional to the ratio between the area of the carbon layer and the area of the hole when the area of the hole is not too small. In other words, within the large hole end, when the ratio of the carbon

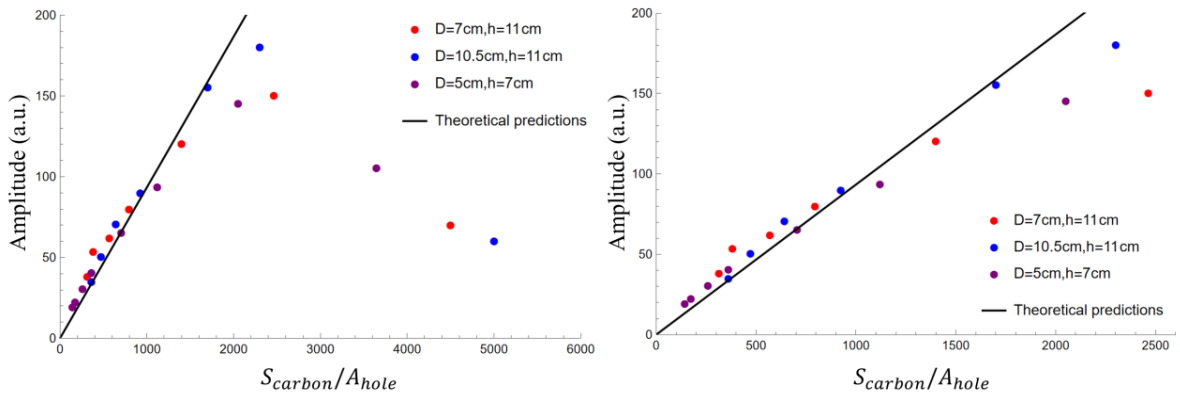


Figure 2.9 Sound intensity vs the ratio of the carbon layer area and the hole area

layer to the hole area increases, the sound intensity increases. This relationship is clearly illustrated in Figure 2.9.

We will provide a semi-quantitative explanation for this phenomenon in the discussion section.

## 2.3 Experiment II: Intensity vs. bulb power

In order to investigate the impact of light intensity on the sound intensity, we have used a voltage transformer to change the voltage of the AC power (Figure 2.10), thus tuning the bulb power. We have also left sufficient time for cooling the tungsten filament between different trials, to ensure the constant experimental condition of the bulb.

Figure 2.10 Experimental setup with the voltage transformer.

| $D$(cm) | $h$(cm) | $d$(mm) | Voltage(V) | Sound intensity (a. u. ) |
|---|---|---|---|---|
| 7 | 11 | 2.5 | 100 | 13.6 |
| | | | 120 | 22.9 |
| | | | 140 | 25.1 |
| | | | 160 | 50.9 |
| | | | 180 | 77.9 |
| | | | 200 | 122.8 |
| | | | 220 | 145.3 |
| 10.5 | 11 | 5 | 100 | 9.3 |
| | | | 120 | 15.7 |
| | | | 140 | 18.1 |
| | | | 160 | 40.2 |
| | | | 180 | 65.7 |
| | | | 200 | 84.1 |
| | | | 220 | 131.3 |
| 5 | 7 | 2.5 | 100 | 7.2 |
| | | | 120 | 18.3 |
| | | | 140 | 20.0 |
| | | | 160 | 29.9 |
| | | | 180 | 43.4 |
| | | | 200 | 72.1 |
| | | | 220 | 121.1 |

Table 2.2 Experimental data

After repeating these experiments for multiple trials, the experimental data turned out to take on a regular pattern and match intuitive expectations with a reasonable error. There is a positive correlation between the sound intensity and the voltage applied to

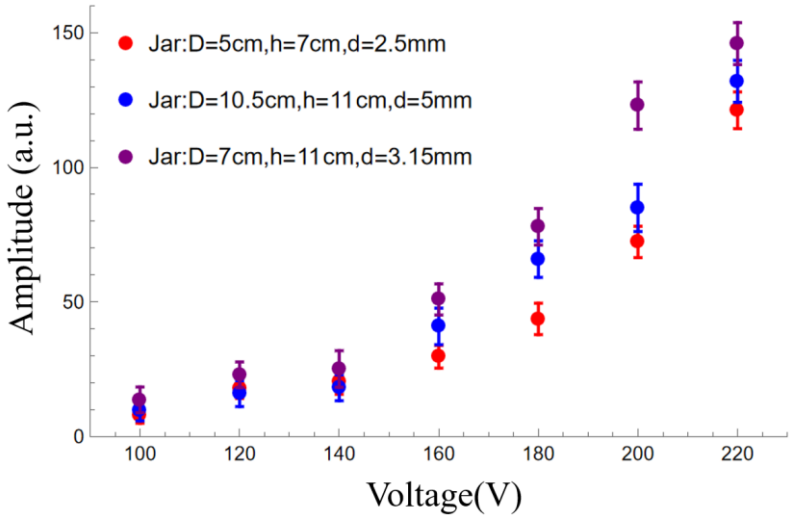


Figure 2.11 Experimental data.

the tungsten as shown in Figure 2.11, which will be quantitatively manifested in the

discussion section.

## 2.4 Experiment III: Intensity vs. Distance

Here, we have adjusted the distance from the tungsten filament to the carbon layer in the jar. Intuitively, as the distance increases, the power of the light received by the carbon decreases, thus the sound intensity will decrease at the same time.

| Distance (cm) | Sound intensity (a. u.) |
|---|---|
| 11 | 38.4 |
| 12 | 32.0 |
| 13 | 30.2 |
| 15 | 29.8 |
| 17 | 22.4 |
| 20 | 14.6 |
| 23 | 9.0 |
| 26 | 9.0 |
| 32 | 5.7 |

Table 2.3 Experimental data

In this experiment, we have chosen the jar whose diameter is 7 cm and height with carbon is 11 cm. The hole on the cap is 0.25 cm. We can extract the amplitude of the sound at 100Hz as shown in Table 2.3 and Figure 2.12.

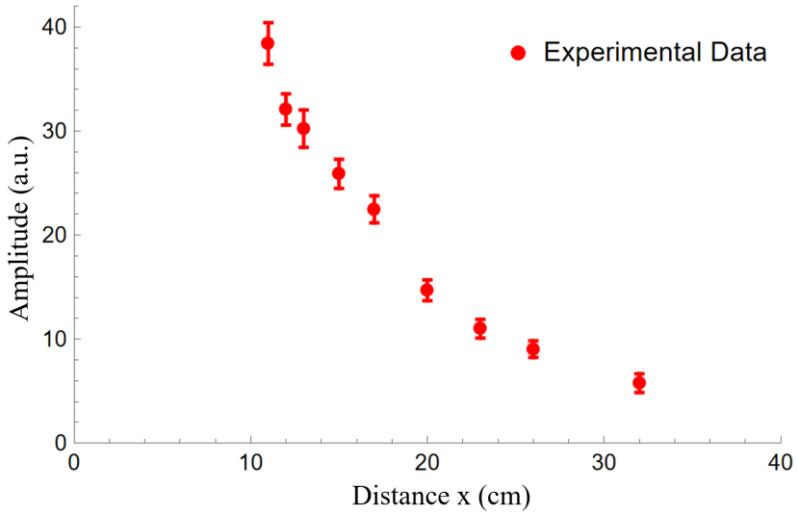


Figure 2.12 Amplitude vs. Distance

The amplitude of the sound is decreasing when the distance is increasing. This decreasing trend will be quantitatively discussed in the discussion part.

# III. Theory and Modeling

## 3.1 Qualitative explanation of the phenomenon

In this part, we are going to give a qualitative analysis of the incident light, changing temperature of the carbon layer and the adjacent air, and the movement of the air. As shown in Figure 3.1, the key physical principle that makes this phenomenon happen is photoacoustic effect.

Since the voltage of the AC power is changing throughout time $(1\omega)$, the heating power of the voltage is also changing with a double frequency $(2\omega)$ because of the Joule's Law $(P = V^2/R)$. Such electric power will heat up the tungsten filament. Thus, the temperature of the filament will various at a frequency of 100 Hz $(2\omega)$. Using the theory of the Blackbody radiation, the light intensity of the bulb has a linear relationship with the tungsten temperature. Thus, the intensity of the emitted light oscillates at a frequency of 100 Hz $(2\omega)$ too. The light will be absorbed by the carbon layer and heat it up. Since the carbon layer has very poor thermal conductivity, its temperature oscillates as the light intensity of 100 Hz $(2\omega)$. Meanwhile, the heat of the carbon layer will be transmitted to a thin layer of air in front of it. The oscillating air temperature will make its volume change according to the ideal gas law at a frequency of 100 Hz $(2\omega)$. The air then can act as a piston which pushes

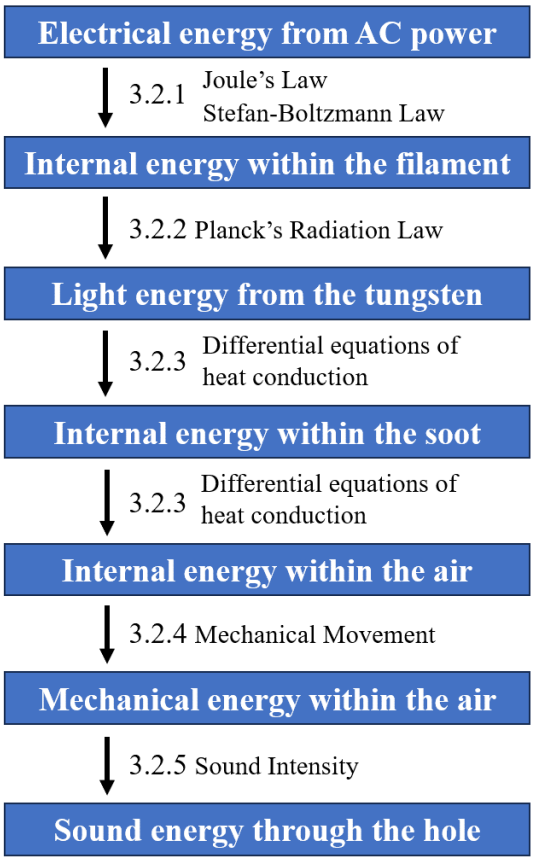


Figure 3.1: Mind map of quantitative analysis

the other air in the jar moving in and out of the jar through the hole. Finally, such mechanical movement produces a sound at 100Hz.

## 3.2 Quantitative analysis

### 3.2.1 Time dependent filament temperature

The voltage of the household power is changing as a sine wave shown in Figure 3.2, at a frequency of 50 Hz. $\widetilde{U}$ is the AC voltage of the power, and $\omega$ is the angular frequency of the voltage.

$$\widetilde{U} = U_0 \sin \omega t \tag{3.1}$$

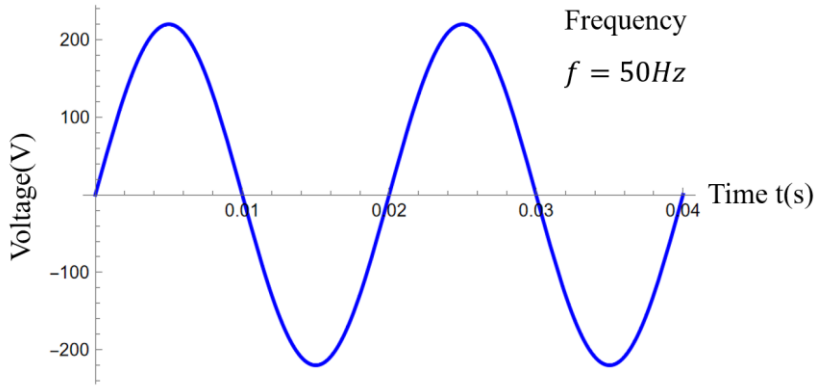


Figure 3.2 The sine wave of the voltage from an AC power

The AC power heats the tungsten filament, and the Joule's Law can be used to calculate the heating power received by the tungsten filament.

$$P_{bulb} = \frac{\widetilde{U}^2}{R} = \frac{U_0^2 \sin^2 \omega t}{R}$$

$$P_{bulb} = \frac{U_0^2}{2R}(1 - \cos 2\omega t) \tag{3.2}$$

Then we can acquire the power of the light bulb through time using Equation 3.2 as shown in Figure 3.3. Here we can see that that the heating power is double the frequency of the AC power, which is 100 Hz.

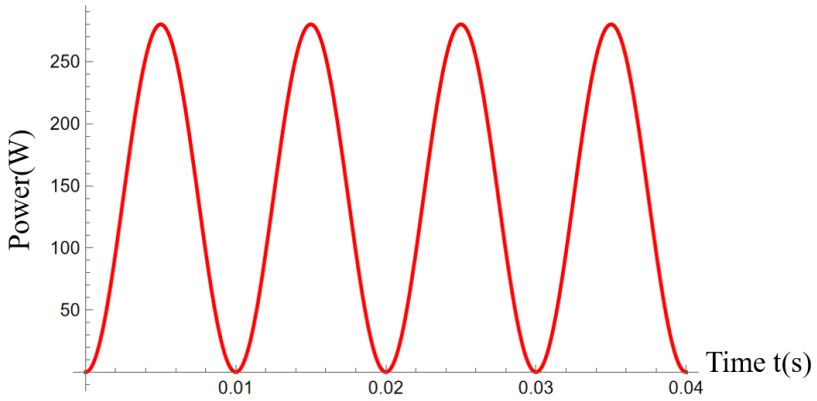


Figure 3.3 Sine wave of the heating power from an AC power

If we normalize the amplitude of the voltage and the power into 1, we can get Figure 3.4, which shows a clear trend of the double frequency of the power.

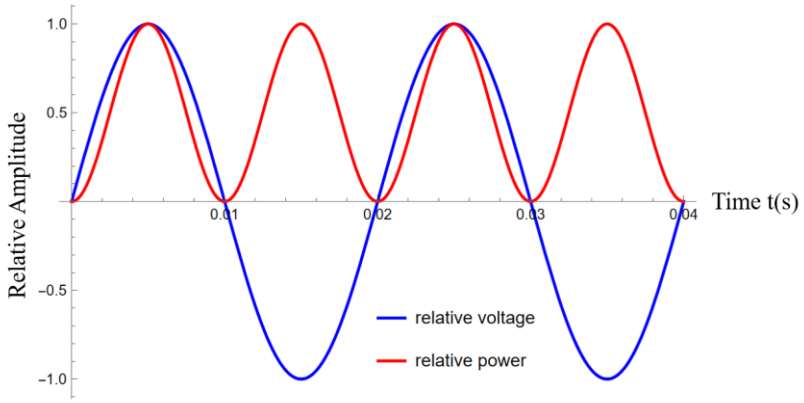


Figure 3.4 Normalized waves of the AC voltage and the heating power.

Then we can delve into the discussion of the temperature of the filament. The function describing the temperature increasement of the tungsten filament is:

$$Q_c = c_t \cdot \Delta T \tag{3.3}$$

There, $c_t$ is the total heat capacity of it. The power absorbed by the tungsten $Q_c$ is equal to the power produced by the $P_{bulb}$ minus the power emitted away in the form of light $P_{emission}$. Here we have ignored the heat conduction, since the filament is mounted inside a vacuum bulb. The power emitted in the form of light can be measured with Stefan-Boltzmann law, where $\sigma$ is the Stefan constant, $S$ is the surface area of the tungsten filament.

$$Q_c = P_{bulb} - P_{emission} \tag{3.4}$$

$$c_t \cdot \frac{dT}{dt} = \frac{U_0^2}{2R}(1 - \cos 2\omega t) - \sigma S \cdot T^4 \tag{3.5}$$

Solving the differential equation 3.5 numerically, we are able to find that the temperature is actually changing in the frequency of 100Hz and almost remain the same after initial heating up (Figure 3.5). As shown in Figure 3.5 right, the oscillation frequency of 100 Hz and amplitude of 2ΔT=44 K can be observed clearly.

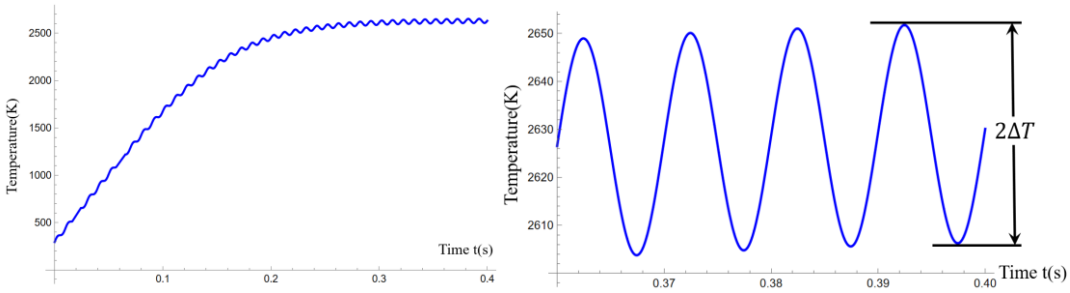


Figure 3.5: Time-dependent temperature of the tungsten filament.

Thus, we can rewrite the temperature into two part: a time independent part and an oscillating part.

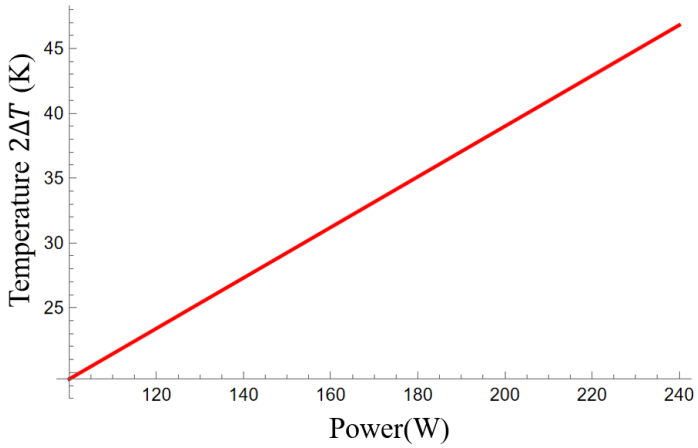


Figure 3.6: oscillation amplitude changing with heating power

$$T = T_0 + \Delta T \sin 2\omega t \tag{3.6}$$

By simulation, we have also found that the oscillation amplitude has a linear relationship with the heating power, as shown in Figure 3.6. Thus,

$$\Delta T \propto P_{bulb} \propto U^2 \quad 3.7$$

### 3.2.2 Light emitted from the filament

Since the light emitted by the tungsten filament is thermally emitted, the light intensity then depends on the temperature of the filament. Here we have taken the assumption of black body radiation:

$$L(\lambda, T) = \frac{2hc}{\lambda^3} \frac{1}{e^{\frac{hc}{k_b \lambda T}} - 1} \quad 3.8$$

Where $h$ is Plank's constant, $c$ is the speed of light, $k_b$ is Boltzmann's constant.

However, the real spectral radiance of the tungsten needs to multiplying the spectral emissivity of the tungsten $\varepsilon(\lambda, T)$:

$$L_{eff}(\lambda, T) = L(\lambda, T) \cdot \varepsilon(\lambda, T)$$

$\varepsilon(\lambda, T)$ can be simplified into the formula below [3]:

$$\varepsilon(\lambda, T) \approx 0.4655 + 0.01558\lambda + 0.2675 \times 10^{-4} T - 0.7305 \times 10^{-4} \lambda T \quad 3.9$$

Thus, we can get the complete expression of the effective spectral radiance of the tungsten:

$$L_{eff}(\lambda, T) \approx \frac{3.975 \times 10^{-25} \times (0.4655 + 0.01558\lambda + 0.2675 \times 10^{-4} T - 0.7305 \times 10^{-4} \lambda T)}{\lambda^3 (e^{\frac{hc}{k_b \lambda T}} - 1)} \quad 3.10$$

Integrate the effective spectral radiance in all the wave length, we are able to get the total spectral radiance $I_T$:

$$I_T(T) = \int_0^{+\infty} L_{eff}(\lambda, T)\, d\lambda \quad 3.11$$

When emitting the photon and producing light, the temperature of the tungsten is in the interval (2500K, 3000K). As shown in Figure 3.7, the total spectral radiance $L_T$ is approximately linear with the filament temperature.

$$I_{light} \propto T \quad 3.12$$

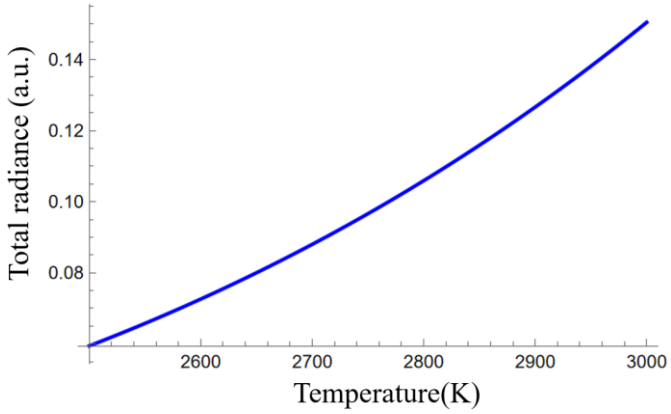

Figure 3.7: Total spectral radiance of tungsten

As discussed before, since the filament temperature oscillates at a frequency of 100Hz, the intensity of emitted light also oscillates at the same frequency. As a result, we can define the light intensity in a similar way as the tungsten's temperature in Equation 3.6:

$$I_{light} = I_{DC} + I_{AC} \sin 2\omega t \qquad 3.13$$

Here, both $I_{AC}$ and $I_{DC}$ are constant for fixed bulb power, and $I_{DC}$ is much larger than $I_{AC}$. Thus,

$$I_{AC} \propto \Delta T \propto U^2 \qquad 3.14$$

After the light is emitted, a fixed portion of it (depending on the distance between the filament and the carbon layer) shins onto the carbon layer and is absorbed by it. To demonstrate the change of light intensity when passing through the layer of carbon, we use Lambert-Beer Law that helps to quantify the decrease of light intensity when the light is going deeper into a certain material, which states that:

$$\frac{dI_{light}}{dx} = -\beta I_{light}$$

where $\beta$ is the optical absorption coefficient.

Using a different way to express it by substituting $I_{light}$ by Equation 3.13, we obtain the light intensity observed per unit length:

$$\frac{dI_{light}}{dx} = -\beta e^{-\beta x}(I_{DC} + I_{AC} \sin 2\omega t). \qquad 3.15$$

### 3.2.3 Time dependent temperature of the carbon layer and the adjacent air

Now, we are going to construct a set of partial differential equations to quantitatively describe the heat transformation from the light to the carbon, and to the air. Here, Fourier's law of heat conduction is applied to depict the temperature field, with the assumption of a one-dimensional problem (since the situation is identical across every cross section, the sufficiency is clear).

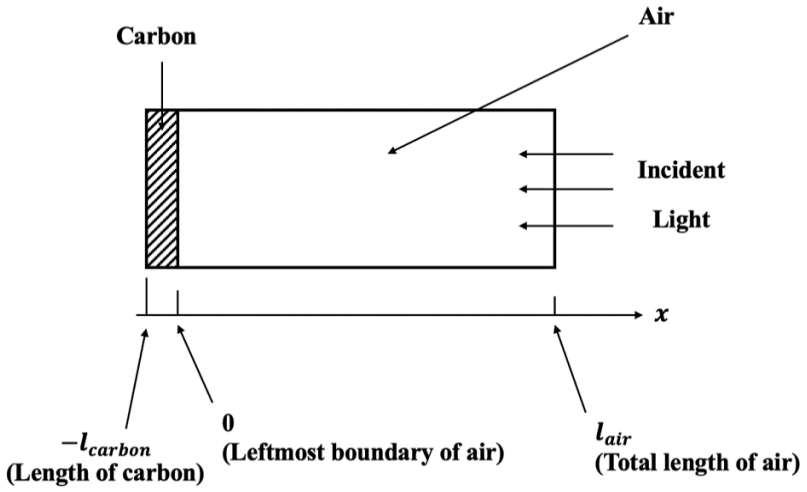


Figure 3.8 The schematic diagram of the jar and the coordinate.

According to Figure 3.8, the heat conduction equations and boundary conditions can be easily written as follows.

For the carbon, $T_{carbon}$ is the temperature of the carbon and $\alpha_{carbon}$ is the thermal diffusivity of the carbon. Here $k_{carbon}$ is the thermal conductivity of the carbon, $c_{carbon}$ is the specific heat capacity, $\rho_{carbon}$ is the density of the carbon, and $\rho_{carbon}c_{carbon}$ is the volumetric heat capacity of the carbon. There is heat transferring from the light to the carbon and from the carbon to the air, so the Furrier heat transforming formula is used.

$$\frac{\partial T_{carbon}}{\partial t} = \alpha_{carbon} \frac{\partial^2 T_{carbon}}{\partial x^2}$$

$$\alpha_{carbon} = \frac{k_{carbon}}{\rho_{carbon} c_{carbon}}$$

There are always heat transferred from the light at a frequency of $2\omega$. As a result, the term of the absorption of energy transmitted from light is added, then the heat conduction equation above is modified into the formula below, where $k_{carbon}$ is the thermal conductivity of the carbon.

$$\frac{\partial T_{carbon}}{\partial t} = \alpha_{carbon} \left( \frac{\partial^2 T_{carbon}}{\partial x^2} + \frac{1}{k_{carbon}} \beta e^{-\beta x} (I_{DC} + I_{AC} \sin 2\omega t) \right) \quad 3.16$$

Similarly, we can get the equation, where $\alpha_{air}$ is defined similarly to $\alpha_{carbon}$.

$$\frac{\partial T_{air}}{\partial t} = \alpha_{air} \frac{\partial^2 T_{air}}{\partial x^2} \quad 3.17$$

We can use the continuity function of temperature and heat-flux at the air-carbon boundary to set up the boundary condition equations:

$$T_{air}(0,t) = T_{carbon}(0,t) \quad 3.18$$

$$k_{air} \frac{\partial T_{air}}{\partial x}(0,t) = k_{carbon} \frac{\partial T_{carbon}}{\partial x}(0,t) \quad 3.19$$

Using the Equations of 3.16, 3.17, 3.18 and 3.19, the solutions describing the time-dependent temperature of the carbon and the air is obtained as below:

$$T_{carbon}(x,t) = T_{room} + \left(1 - \frac{e^{-\beta x}}{l_{carbon(eq)}}\right) \xi_{carbon} + \psi_{carbon} e^{-\beta x} \left(\cos(2\omega t) + \boldsymbol{i} \sin(2\omega t)\right) \quad 3.20$$

$$T_{air}(x,t) = T_{room} + \left(1 - \frac{x}{l_{air}}\right) \xi_{air} + \psi_{air} e^{-a_{air} x} \left(\cos(2\omega t - a_{air} x) + \boldsymbol{i} \sin(2\omega t - a_{air} x)\right) 3.21$$

$$l_{carbon(eq)} := \frac{\beta k_{carbon}}{c_{carbon} m_{carbon}}$$

$$a_{air} := \sqrt{\frac{\omega}{\alpha_{air}}}$$

$T_{room}$ is the room temperature, $l_{air}$ is the characteristic length of the air inside the jar, $l_{carbon(eq)}$ is the characteristic length of the carbon, $a_{air}$ is the equivalent attenuation

coefficient of the air. $\xi_{carbon}$ is the moduli of the time-independent term, here

$$\xi_{carbon} = \xi_{air} := \frac{I_{DC}}{c_{carbon} m_{carbon}}$$

Where $c_{carbon}$ is the specific heat of the carbon and $m_{carbon}$ is the mass of the carbon.

The amplitude of the periodic variation $\psi_{carbon}$ and $\psi_{air}$ are expressed as below:

$$\psi_{carbon} := \frac{\beta I_{AC}}{2k_{carbon}(\alpha_{carbon}\beta^2 - \omega)}$$

$$\psi_{air} := I_{AC} \frac{\beta\left(\beta I_{DC} k_{carbon} l_{carbon(eq)} l_{air} - \beta k_{carbon}\left(k_{carbon}\xi_{air} l_{carbon(eq)} + k_{carbon} l_{air}\right)\right)}{2(\alpha_{carbon}\beta^2 - \omega)\left(k_{air} a_{air} I_{DC} l_{carbon(eq)} k_{carbon} l_{air} - \beta k_{carbon}\left(k_{carbon}\xi_{air} l_{carbon(eq)} + k_{carbon} l_{air}\right)\right)}$$

$$\psi_{air} \propto I_{AC} \qquad 3.22$$

It is important to mention that the quantities $\psi_{carbon}$ and $\psi_{air}$ are only dependent on the physical properties of the carbon and air, and independent of time$(t)$ and position$(x)$.

It is clear that the expression describing $T_{air}$ (Equation 3.21) can be divided into three parts. First term is the initial room temperature. Second term is linearly dependent on the position x, which describes simply the thermal conductance of the heat from the high temperature end (carbon layer) to infinite position. This term is time-independent. And the third term describes the periodically variative time-independent AC part. Here, $\psi_{air}$ is independent of x and t and proportional to the oscillating light intensity $I_{AC}$. $e^{-a_{air}x}$ is the attenuation function of $x$ (here $a_{air}$ is the decay constant associated with the frequency and the thermal diffusivity of the air). $\cos(2\omega t - a_{air}x) + \boldsymbol{i}\sin(2\omega t - a_{air}x)$ is the periodic variation with a frequency of 2ω. This term is also related to the position.

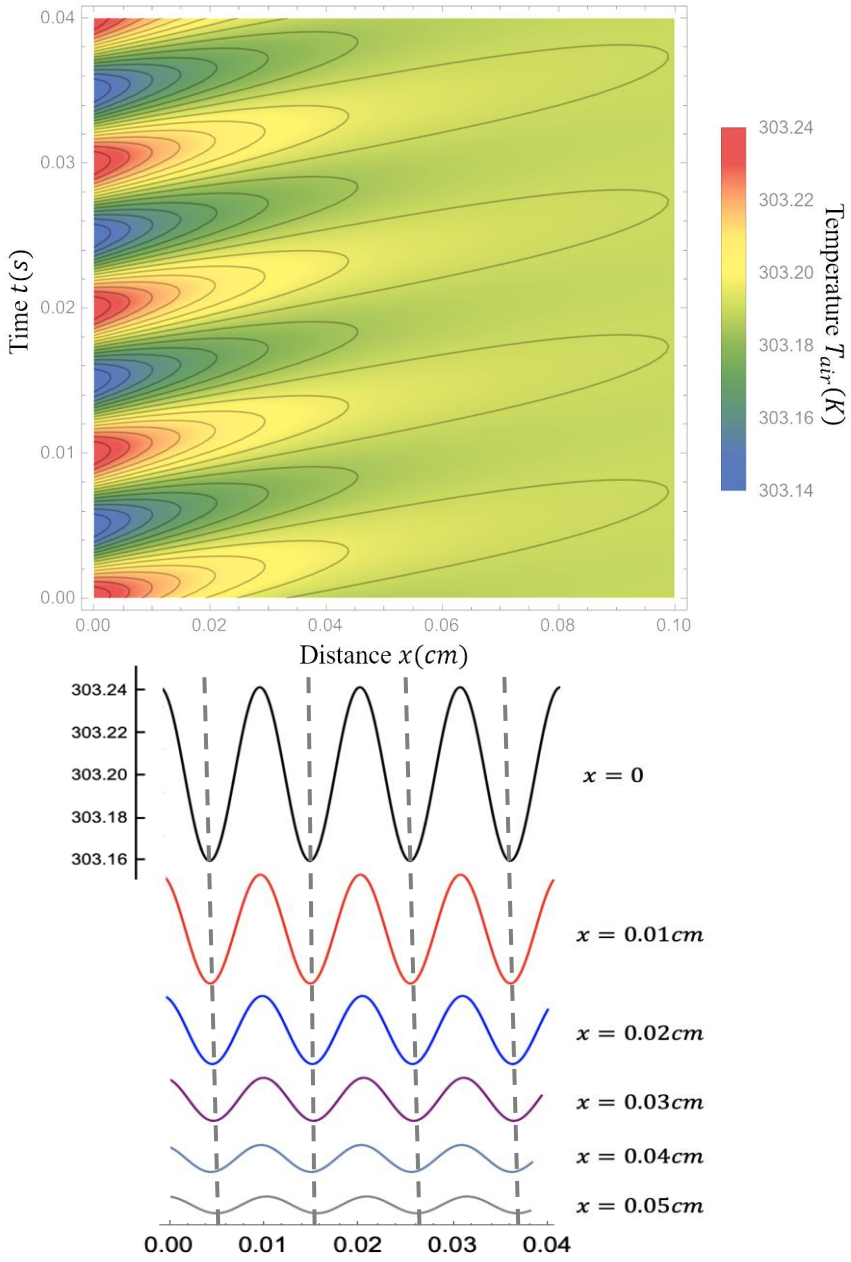


Figure 3.9 Temperature of the adjacent air vs. time and position.

Figure 3.9 exhibits the temperature field of the air near the carbon using the theoretical result we gotten by solving the differential equations, where x=0 represents the carbon-air boundary shown in Figure 3.8. The temperature at position x=0 modulates at a frequency of 2ω (100Hz), the same as the frequency of $I_{AC}$ (Equation 3.13). We have also noticed that the heat is spreading towards outer place throughout time and the peak almost disappears at 1mm away from the carbon layer.

Thus, we are able to conclude that the frequency of the temperature vibration of the air equals to the frequency of the oscillating light intensity at 100 Hz.

### 3.2.4 The mechanical movement of the air piston

During the process, the temperature of the air oscillates due to the oscillating light ($I_{AC}$), which makes the air expand and shrink. Because the oscillating frequency $f \gg$ 10Hz, the volume of the air V changes rapidly and heat conduction can be ignored. Thus the air's expansion or contraction can be treated as in an adiabatic process.

According to the ideal gas law and Gas adiabatic equation:

$$pV = nRT \tag{3.23}$$

$$pV^{\gamma} = const \tag{3.24}$$

$V$ and $T$ have the following relationship:

$$V^{\gamma-1}T = const \tag{3.25}$$

Differentiate equation 3.25:

$$T(\gamma - 1)V^{\gamma-2}dV + V^{\gamma-1}dT = 0 \tag{3.26}$$

$$dT = -T(\gamma - 1)\frac{dV}{V} = -T(\gamma - 1)\frac{\partial \xi_{vib}}{\partial x} \tag{3.27}$$

Integrate equation 3.27:

$$\int dT \propto \int \frac{\partial \xi_{vib}}{\partial x} \tag{3.28}$$

Thus:

$$\xi_{vib} \propto \Delta T_{air} \tag{3.29}$$

Thus, the oscillating amplitude of the "Air piston" is proportional to the oscillating temperature of the "adjacent Air" $\Delta T_{air}$ （Figure 3.10）.

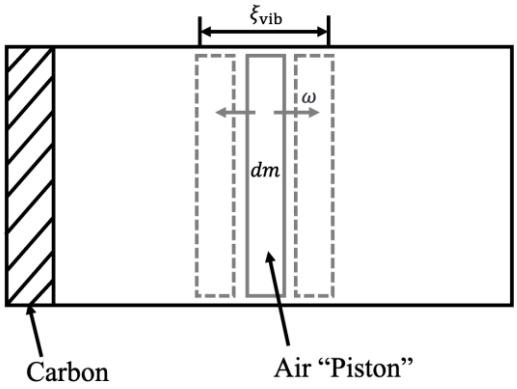


Figure 3.10. The schematic diagram of the vibration of the air "piston".

### 3.2.5 The sound intensity

We first analyze a mass unit having an oscillation displacement:

$$\xi = \xi_{vib}\cos\left(\omega(t-\frac{x}{u})\right) \tag{3.30}$$

The mass unit has kinetic energy and potential energy.

The kinetic energy can be written as:

$$dE_k = \frac{1}{2}\rho_{air}(dS\cdot dx)\left(\frac{\partial\xi}{\partial t}\right)^2 = \frac{1}{2}\rho_{air}\omega^2\xi_{vib}^2\sin^2\left(\omega\left(t-\frac{x}{u}\right)\right)dV \tag{3.31}$$

The potential energy can be written as:

$$dE_p = \frac{1}{2}k_{dx}[\xi(x+dx,t)-\xi(x,t)]^2 = \frac{1}{2}\rho_{air}\omega^2\xi_{vib}^2\sin^2[\omega\left(t-\frac{x}{u}\right)]\,dV \tag{3.32}$$

All the oscillating mass units possess kinetic energy and potential energy which distribute in the space.

The energy density in the space can be written as:

$$\varepsilon = \frac{d(E_k+E_p)}{dV} = \rho_{air}\omega^2\xi_{vib}^2\sin^2[\omega\left(t-\frac{x}{u}\right)] \tag{3.33}$$

We take the time average value of the energy density:

$$\overline{\varepsilon} = \frac{d(E_k+E_p)}{dV} = \frac{1}{2}\rho_{air}\omega^2\xi_{vib}^2 \tag{3.34}$$

The energy going through a unit area $dS$ in a small-time section $dt$:

$$dE = \varepsilon(v_{sound}dt)dS \tag{3.35}$$

Consequently, the energy flux is:

$$i = \frac{dE}{dtdS} = \varepsilon v_{sound} \tag{3.36}$$

Sound power is:

$$P_{sound} = \bar{i} S_{carbon} = \bar{\varepsilon} v_{sound} S_{carbon} = \frac{1}{2} \rho_{air} \omega^2 \xi^2 v_{sound} S_{carbon} \tag{3.37}$$

Finally, the sound intensity/energy flux near the hole is:

$$I_{sound} = \frac{\overline{dE}}{dt} \cdot \frac{1}{dS} = \frac{P_{sound}}{A_{hole}} = \frac{\frac{1}{2} \rho_{air} \omega^2 \xi_{vib}^2 v_{sound} S_{carbon}}{A_{hole}} \tag{3.38}$$

Thus,

$$I_{sound} \propto \frac{S_{carbon}}{A_{hole}} \cdot \xi_{vib}^2 \tag{3.39}$$

$$I_{sound} \propto \xi_{vib}^2 = \Delta T_{air}^2 \tag{3.40}$$

Here, we have the conclusion that the sound intensity is proportional to the density of the air, the square of the AC frequency, the area of the carbon, and inversely proportional to the hole size. And we also have the sound intensity is proportional to the ratio of $\frac{S_{carbon}}{A_{hole}}$.

# IV. Discussion

## 4.1 Discussion of Experiment I: hole diameter

Figure 4.1 exhibits the sound intensity vs the ratio of the area of the carbon layer to hole area. Clearly, at low horizontal axis region, the sound intensity approximately scales linearly with the ratio, as indicated by the black solid line. These data agree well with the theoretical prediction, as Equation 3.33:

$$I_{sound} \propto \frac{S_{carbon}}{A_{hole}}$$

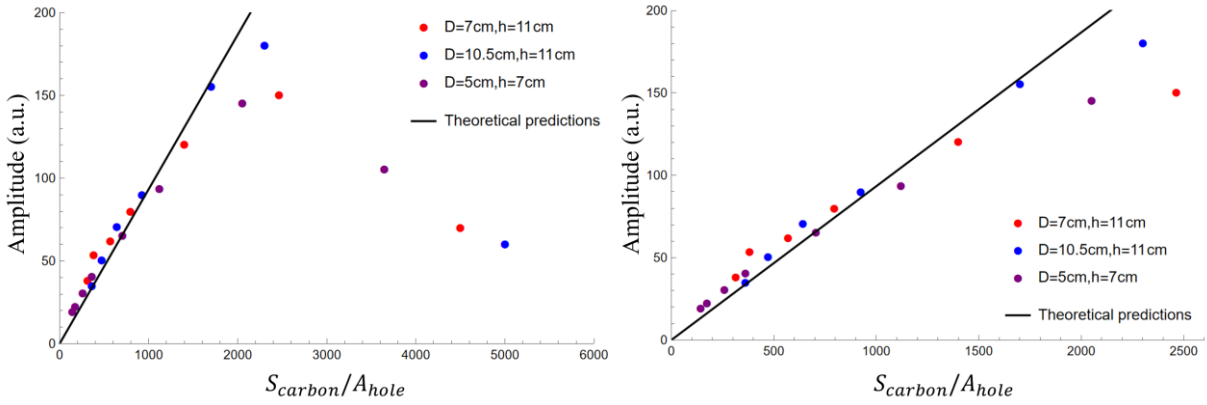


Figure 4.1 Comparison of the theoretical prediction and the experimental result.

On the higher region of the horizontal axis, corresponding to very small holes, the sound intensity decreases rapidly. This can be understood as that excessively small holes pose significant resistance to the inflow and outflow of air. Furthermore, air encounters protrusions along the hole edges, inducing turbulence. This effect becomes more pronounced as the hole size decreases, further diminishing the sound intensity.

## 4.2 Discussion of Experiment II: light intensity

From the previous discussion, we have Equation 3.34:

$$I_{sound} \propto \xi_{vib}^2$$

Here the maximum displacement of the piston air, can be represent by the amplitude of the oscillating $x(t)$, which is $\Delta x$. Thus, including 3.14, 3.24, 3.25, we can get:

$$\xi_{vib} = \Delta x \propto \Delta V \propto \Delta T \propto I_{AC} \quad 4.1$$

$$I_{sound} \propto \xi_{vib}^2 \propto I_{AC}^2 \propto U^4 \quad 4.2$$

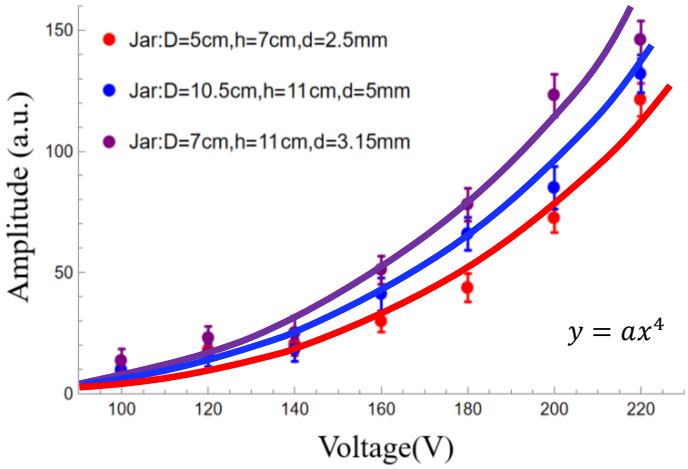


Figure 4.2 Amplitude vs. AC voltage. The solid lines are the fitting results of 4th power law.

Using the relationship mentioned above, the experimental data can be fitted by a 4th power law, as shown in Figure 4.2. The experimental data show a strong agreement with the theoretical model.

## 4.3 Discussion of Experiment III: distance

In order to quantitatively discuss this parameter, we treat the filament to be a point light source, considering the length of filament (~2 cm) is much smaller than the distance x (~20cm). Since the tungsten filament emits light at all the direction, we can conduct a sphere to represent the light emitted by the bulb. The area covered with carbon only absorbed part of the light. As a result, if we project the carbon layer to the sphere, we are able to find out how much portion of the light has been absorbed by the

carbon.

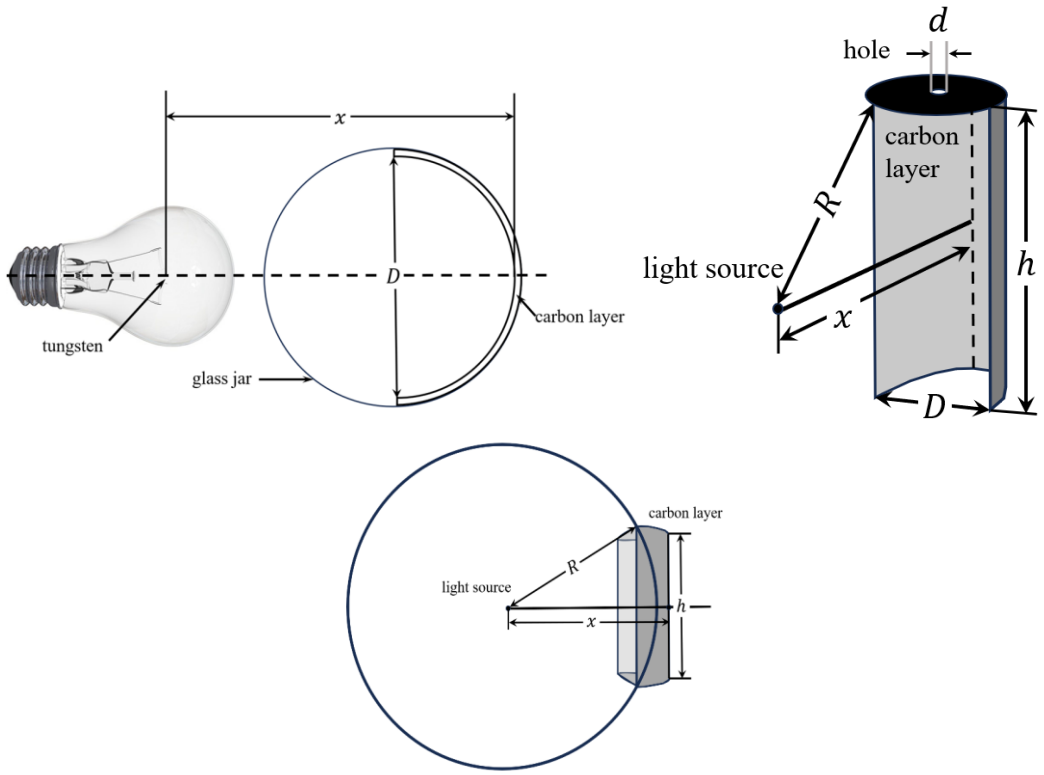


Figure 4.3 Schematic diagram of the sphere and the carbon layer

The diagram of the sphere is shown in Figure 4.3. We can use the distance between the one of the four vertexes and the light source as the radius of the sphere. According to the inner geometric of the jar (D = 7 cm, h = 11 cm), we are able to express the radius of the sphere as Equation 4.3, where $x$ is the distance between the light source and the farthest point of carbon, $D$ is the diameter of the jar, and $h$ is the height of the jar covered with carbon:

$$R = \sqrt{\frac{D^2+h^2}{4} + \left(x - \frac{D}{2}\right)^2} \qquad 4.3$$

The percentage of the light absorbed by the carbon layer can be calculated using a solid angle in such sphere. We first define angle α, β, and γ as shown in Figure 4.4:

$$\alpha = 2\sin^{-1}\frac{h}{2R} \qquad 4.4$$

$$\beta = 2\sin^{-1}\frac{D}{2R} \quad 4.5$$

$$\gamma = 2\sin^{-1}\frac{\sqrt{h^2+D^2}}{2R} \quad 4.6$$

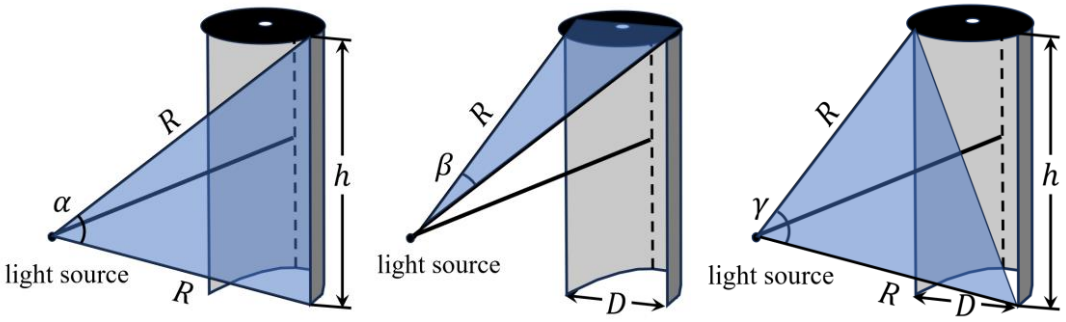


Figure 4.4 Schematic diagram of the angle α, β, and γ.

Using α, β, and γ, we can get the formula of solid angle of the rectangular carbon layer Ω as shown below:

$$S = \frac{1}{2}(\alpha + \beta + \gamma) \quad 4.7$$

$$\Omega = 8\tan^{-1}\sqrt{\tan\frac{S}{2}\cdot\tan\frac{S-\alpha}{2}\cdot\tan\frac{S-\beta}{2}\cdot\tan\frac{S-\gamma}{2}} \quad 4.8$$

Ω represents the portion of the light been observed by the carbon. The absorbed light intensity can be represented as $\frac{I_{AC}}{4\pi}\cdot\Omega$. Since the light intensity has a quadratic relationship with the sound intensity (Equation 4.2), we can calculate the $I_{sound}$ by using $I_{light}^2$.

$$I_{sound} \propto I_{AC}^2$$

$$I_{sound} \propto \left(\frac{I_{AC}}{4\pi}\cdot\Omega\right)^2 \quad 4.9$$

For a particular experiment, $I_{AC}$ is constant. The fitting result using the Equation 4.9 and 4.8 is shown in Figure 4.6. In the fitting model, $a = \left(\frac{I_{AC}}{4\pi}\right)^2 = 268$, and the fitting has an $r^2 = 0.967$, representing that it is a good fit.

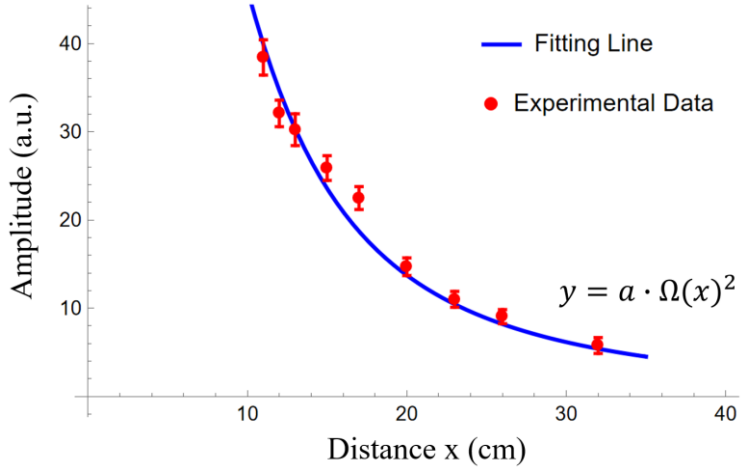


Figure 4.5 Fitted result.

From Figure 4.5, we are able to find out that the amplitude of the sound is decreasing in respond to the growing of distance. Such trend is caused by the smaller percentage of the light absorbed by the carbon when the distance grows larger.

# V. Conclusion

In summary, we have set up an experiment “hearing light” to test the phenomena of photoacoustic effect. We have constructed a physical model to quantitatively analyze the relationship between the sound intensity and other geometric factors, such as the power of the light bulb (AC voltage), the distance and the diameters of the holes. In the process, we have accomplished:

1. Experiments have been successfully and systematically performed, and quantitative data have been acquired.

2. A quantitative theoretic model have been constructed including black body radiation theory, secondary differential equations of thermal conduction and ideal gas law. Most importantly, the prediction of the theoretic model has been confirmed by the experimental data.

3. We have found: a) the frequency of the sound is double of that of the AC power; b) the intensity of the sound is linearly proportional to the light intensity. c) in surprise, the intensity of the sound is linearly proportional to the ratio of the area of the carbon layer to the area of the hole.

In the future, we are going to make our experiments much more completely in the following ways:

1. Build up a quieter environment with sound absorbing material.
2. Analyze the influence of the frequency of the AC power.
3. Build a stimulation model for the temperature field on COMSOL.
4. Discuss the influence of different jar shapes instead of using only cylinder and hexagonal prism shape jars.

# VI. Reference

[1] Bell, A. G. (1880). ART. XXXIV.--On the production and reproduction of sound by light. *American Journal of Science* (1880-1910), 20(118), 305.

[2] Rosencwaig, A., & Gersho, A. (1975). Theory of the photoacoustic effect with solids. *The Journal of the Acoustical Society of America*, 58(S1), S52–S52.

[3] Larrabee, R. D. (1959). Spectral emissivity of tungsten. JOSA, 49(6), 619-625.

[4] Arnold, H. D., & Crandall., I. B. (1917). The Thermophone as a Precision Source of Sound. *Physical Review*, 10(1), 22–38.

[5] Hamasha, K. M., & Arnott, W. P. (2009). Photoacoustic measurements of black carbon light absorption coefficients in Irbid city, Jordan. *Environmental Monitoring and Assessment*, 166(1-4), 485–494.

[6] Khizhnyak, P. E., Chechetkin, A. V., & Glybin, A. P. (1979). Thermal conductivity of carbon black. *Journal of Engineering Physics*, 37(3), 1073–1075.

# VII. Acknowledgement

It is a significant and unforgettable experience for us to spend such a long time on writing, modifying and polishing this paper. We would like to give our heartfelt thanks to Professor He Liang from Nanjing University, whose rigorous academic attitude and spirit of striving for excellence have always infected us. Professor He attached great importance to cultivating our scientific research habits. We felt confused about this in the beginning. However, after experiencing countless setbacks and failures in experiments, we realized the importance of collecting data and keeping detailed experimental records. We deeply understood Professor He's repeated emphasis on good research habits. These research habits will benefit us for a lifetime.

The three of us worked closely during the research process. Facing countless failures and setbacks, we encouraged each other and overcame multiple difficulties together. Zhou Yincheng was responsible for simulation modeling and experiments. Wang Xiaoyuan was responsible for mathematical modeling. Wang Shi was responsible for formula derivation. The three of us wrote our research contents respectively. Zhou Yincheng was responsible for summarizing all the contents and compiling the paper.

# VIII. Team Member's Information

Name: Zhou Yincheng

Gender: Male

School: Nanjing Foreign Language School

Grade: Senior

Introduction: Enjoy finding the beauty of Physics, dream of using physics to make a difference to the world.

Awards: 2023 China Young Physicist Tournament (CYPT2023) National First Place, 2022 British Physics Olympiad Gold, 2023 Physics Bowl Gold，2023 American Regions Mathematics League Nation Top 100

Name: Wang Xiaoyuan

Gender: Male

School: Nanjing Foreign Language School

Grade: Senior

Introduction: Deep interest in physics and scientific research, love to delve into problems

Awards: 2023 Macao Young Physicist Tournament (MYPT2023) First Place, 2023 Physics Bowl Silver, 2023 American Regions Mathematics League Nation Top 100

Name: Wang Shi

Gender: Male

School: Nanjing Foreign Language School

Grade: Senior

Introduction: Enthusiastic in Physics and Mathematics, dare to explore new ground, have the scientific spirit of exploration

Awards: 2023 Chinese Young Physicist Tournament Exchange in Macao Team Gold Prize, the 19th Pan-Pearl River Delta and Chinese Elite Schools Physics Olympiad First Class Award

# IX. Experimental location and time

June 3

Group members discussed to determine the research topic.

June 4

Group members searched for references, learned related theories, and wrote the first draft of the Theory and Modeling part of this paper.

June 10

Group members conducted an experiment at Nanjing University. A plastic bottle covered by Graphene on the inner wall and an incandescent bulb were used to perform the experiment. Sound could not be heard by naked ear. The experiment failed. Group members had a deep discussion and prepared for the next experiment.

June 15

Wang Shi conducted experiments at home. He used jars covered by soot, carbon powder, and electrical black tape on the inner wall. Caps of the jars were drilled into holes of various sizes. Sound could not be received by mobile phone. The experiment failed.

June 28

Group members explored theoretical analysis framework and formula derivation, summarized previous experiments, and went through reasons for failures.

July 10

Zhou Yincheng conducted experiments at home. A transparent glass jar was used to perform the experiment. Half of the jar was covered by carbon particles produced by burning candles. A microphone with a frequency response of 20Hz-18KHz was used for sound reception. With the help of an audio amplifier, a clear image of 100Hz sound was successfully captured, and the amplified 100Hz sound could be heard by naked ear. The experiment was successful for the first time.

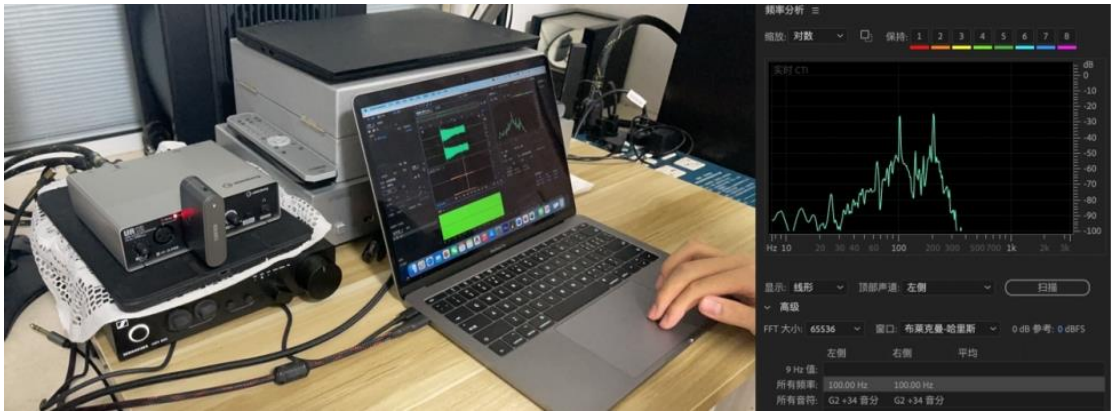

July 12

Group members conducted experiments in a quiet studio. Different parameter variables were set, such as the size of the hole, the power of bulb, the size of the jar, and the distance between light bulb and the carbon layers. Group members recorded the experiment results, extracted data samples, and conducted quantitative analysis.

July 20

Group members conducted experiments using a transformer at Professor He's office. Group members analyzed the impact of changing power of light bulb by adjusting the voltage of transformer.

July 22

Group members discussed the improvement plan of the experiment, revised the experimental verification plan, summarized experiment results and made a comparison between theory and experiment results.

Part of the experiment records are as follows:

| No. | Time | Location | Material | D*h (cm) | Inner attachment | P (W) | d (mm) | Reception device | Result |
|---|---|---|---|---|---|---|---|---|---|
| 1 | June 10 | Nanjing University | Plastic jar | water bottle | Soot | 200 | 2 | Naked ear | Failed |
| 2 | June 15 | Home | Plastic jar | 8*8.5 | Carbon particles | 200 | 3 | Mobile phone | Failed |
| 3 | June 15 | Home | Plastic jar | 8*8.5 | Graphene | 200 | 3 | Mobile phone | Failed |
| 4 | June 15 | Home | Plastic jar | 8*8.5 | Soot (thin layer) | 200 | 3 | Mobile phone | Failed |
| 5 | June 15 | Home | Plastic jar | 8*8.5 | Soot (thick layer) | 200 | 3 | Mobile phone | Failed |
| 6 | June 17 | Home | PMMA jar | 15*25 | Carbon particles | 200 | 0.5 | Mobile phone | Failed |
| 7 | June 17 | Home | PMMA jar | 15*25 | Graphene | 200 | 0.5 | Mobile phone | Failed |
| 8 | June 17 | Home | PMMA jar | 15*25 | Soot (thin layer) | 200 | 0.5 | Mobile phone | Failed |
| 9 | June 17 | Home | PMMA jar | 15*25 | Soot (thick layer) | 200 | 0.5 | Mobile phone | Failed |
| 10 | June 17 | Home | PMMA jar | 15*25 | Carbon particles | 200 | 1 | Mobile phone | Failed |
| 11 | June 28 | Home | PMMA jar | 15*25 | Black tape | 200 | 0.5 | Mobile phone | Failed |
| 12 | June 28 | Home | PMMA jar | 15*25 | Black tape | 200 | 1 | Mobile phone | Failed |
| 13 | June 28 | Home | PMMA jar | 15*25 | Black tape | 200 | 2 | Mobile phone | Failed |
| 14 | July 10 | Home | Glass jar | 7*12 | Carbon particles | 200 | 2 | Microphone | Successful |
| 15 | July 10 | Home | Glass jar | 7*12 | Carbon particles | 200 | 1 | Microphone | Successful |
| 16 | July 10 | Home | Glass jar | 7*12 | Carbon particles | 200 | 3 | Microphone | Successful |
| 17 | July 10 | Home | Glass jar | 8*17 | Carbon particles | 200 | 2 | Microphone | Successful |
| 18 | July 10 | Home | Glass jar | 8*17 | Carbon particles | 200 | 4 | Microphone | Successful |
| 19 | July 12 | Studio | Glass jar | 7*12 | Carbon particles | 100 | 2 | Microphone | Successful |
| 20 | July 12 | Studio | Glass jar | 7*12 | Carbon particles | 100 | 3 | Microphone | Successful |
| 21 | July 12 | Studio | Glass jar | 6.5*8 | Carbon particles | 200 | 1 | Microphone | Successful |
| 22 | July 12 | Studio | Glass jar | 6.5*8 | Carbon particles | 200 | 2 | Microphone | Successful |
| 23 | July 20 | Nanjing University | Glass jar | 7*12 | Carbon particles | Transformer | 4 | Microphone | Successful |
| 24 | July 20 | Nanjing University | Glass jar | 6.5*8 | Carbon particles | Transformer | 1 | Microphone | Successful |
| 25 | July 20 | Nanjing University | Glass jar | 8*17 | Carbon particles | Transformer | 3 | Microphone | Successful |
| 26 | July 20 | Nanjing University | Glass jar | 8*17 | Carbon particles | Transformer | 5 | Microphone | Successful |